Journal of Applied Research and Technology

www.jart.icat.unam.mx

Journal of Applied Research and Technology 21 (2023) 397-406

Original

Performance analysis on the low-power energy harvesting wireless sensor networks with a novel relay selection scheme

Hoang-Sy Nguyen[a] • Hoang-Phuong Van[b]*

[a]*Becamex Business School, Eastern International University, Binh Duong Province, Vietnam*
[b]*Institute of Engineering and Technology, Thu Dau Mot University, Binh Duong Province, Vietnam*

Received 11 15 2021; accepted 03 21 2022
Available 06 30 2023

Abstract: Simultaneous wireless information and power transfer (SWIPT) has been utilized widely in wireless sensor networks (WSNs) to design systems that can sustain themselves by harvesting energy from the surrounding areas. In this study, we investigated the performance of the so-called low-power energy harvesting (LPEH) WSN. Being different from other studies, we equipped each relay with a battery whose characteristics were described by an on/off (1/0) decision scheme as per the Markov property. In this context, an optimal loop interference relay selection (OPLIRS) was proposed and investigated. Moreover, the crucial role of the log-normal distribution method in characterizing the LPEH WSN's constraints was proven and emphasized. The system performance was evaluated in terms of the overall ergodic outage probability (OP) both analytically and numerically with Monte Carlo simulation. Readers can refer to this paper for guidelines on how to define the network constraints, analytically derive the problems, or use the presented results for possible comparison studies.

Keywords: Wireless sensor network, low-power networks, relay selection, Markov model, outage probability, log-normal fading

*Corresponding author.
E-mail address: phuongvh@tdmu.edu.vn (Hoang-Phuong Van).
Peer Review under the responsibility of Universidad Nacional Autónoma de México.

1. Introduction

Following the advancement of the fifth and upcoming sixth-generation communication, simultaneous wireless information and power transfer (SWIPT) holds its place to be a promising technology for self-sustaining communication systems as it can offer notable system performance gains, indicated by the improvements of spectral efficiency (SE), power consumption, interference management and delay of transmission, thanks to its nature of facilitating simultaneous information and energy transmission Perera et al. (2018), Sidhu et al. (2019), Nguyen et al. (2019). For SWIPT cooperative relaying system, there are in use two major modes: half-duplex (HD) and full-duplex (FD). Specifically, in HD mode, the relay is equipped with one antenna functioning so that the data re-transmission from the source is conducted in dedicated and orthogonal channels Laneman et al. (2004). Meanwhile, in FD mode, a relay is equipped with two antennas to facilitate the data receiving and transmitting in the same time slot and bandwidth. Moreover, it is worth noting that the FD wireless network is praised owing to its ability to double the SE and improve considerably the network throughput in comparison with the HD one.

The combination of FD operating mode in EH relaying networks has been a debatable topic regarding the possibility to sustain themselves when operating FD mode and performing the relaying task. However, to the advancement of the antenna, battery technologies and signal processing capacity, it is reasonable to re-assess the FD-EH relaying networks for the promising benefit that they can offer, as in Zhong et al. (2014), Liu et al. (2016), Zeng and Zhang (2015). Additionally, in Li et al. (2016), the utilization of energy storage can bring in zero diversity gain when the SNR level is high. Remarkably, Zhong et al. (2014) discussed intensively the constraints of FD-EH relaying networks and proved that the system performance in three different transmission modes can be boosted significantly.

To describe the outdoor wireless channel, Rayleigh, Rician and Nakagami-m fading channels have been widely accepted among the network designers, Zhang et al. (2015). However, for indoor scenario, to characterize the shadowing effects caused by the building walls, obstacles and human movements, log-normal is a better choice Laourine et al. (2007), Renzo et al. (2010), Zhu et al. (2017), making it a more suitable candidate for smart homes and Industrial Internet of Things (IIoTs) applications. Besides, it is reasonable to use the current advancement in the relaying network technology to further boost the system performance of the household networks. Indeed, this was proven to provide higher channel capacity and wider network coverage range as well as minimizing the shadowing effect, Zhang et al. (2009). Moreover, equipping more relays in a cooperative relaying system provides more degree of freedom (DoF), which enables the system to combine more independent fading signals from the several relays in operation, hence resulting in higher system performance Foschini (2002).

The above studies have provided a background to develop a so-called low-power energy harvesting (LPEH) wireless sensor networks (WSN), which can counteract the high signal attenuation and noise in household scenarios Rubin et al. (2014), Rabie et al. (2017), Pu et al. (2019).

Although the energy harvested from radio frequency (RF) is relatively low in comparison with other sources such as thermal, solar, etc., it is sufficient for operation of several devices and sensors Assogba et al. (2020). Specifically, authors in Georgiou et al. (2016) attempted to measure the free ambient RF and found out that by densifying the Wi-Fi access points, it is possible to not only power the indoor devices (smoke detectors, wearable electronics, etc.) but also to extend their lifetime via trickle charging. Taking a step further into upgrading the indoor electrical grids, a namely power line communication (PLC) has been investigated, in which wireless devices can exploit the existing electricity cables for the improvement of data transmission and energy efficiency Wu (2015). Regarding the security of the physical layer, the available techniques for wireless network are applicable for PLC as well. For example, a case study of how to utilize jamming technique to guard against eavesdroppers for cooperative PLC networks was presented in Salem et al. (2017). In the household setup, it is highly recommended to utilize log-normal fading channels because other fading channels cannot describe efficiently the fading effects caused by walls, human movement and indoor obstacles Renzo et al. (2008). A number of papers have extensively analyzed the performance of relay-aided EH wireless networks embedded in the PLC using different key parameters and proved that this combination is promising for the future of smart grids and indoor wireless communication Cheng et al. (2013), Ezzine et al. (2015), Rabien et al. (2016), Rabie et al. (2018), Ramesh et al. (2020), which is undeniably powered by the development of LPEH WSN.

Inspired by the aforementioned studies, this manuscript assesses the performance of a relay selection (RS) scheme so-called optimal loop interference relay selection (OPLIRS) in the context of LPEH WSN. Notably, the relays are equipped with batteries and operate with FD-AF protocol. The shadowing effect of the network is characterized by the log-normal fading channels.

2. System models

Fig. 1 below depicts a LPEH WSN including a source (S), an in-between cluster (C) of K cooperative relays (R_i), $(1 \leq i \leq K)$, and a destination (D). As being investigated in da Costa and Aissa (2010), Wang et al. (2011), this setup is typical and appropriate for studying the impacts of RS schemes operating

in the wireless networks. Additionally, the coverage extension scenario is assumed so that the communication between (S) and (D) can be realized only with the help of the intermediate relays Nguyen et al. (2018), Riihonen et al. (2011). Besides, the solution can help to overcome the deep shadowing effects as well caused by the movement of human or obstacles in the surrounding area, making it more suitable for the in-studied LPEH WSN, da Costa and Aissa (2010).

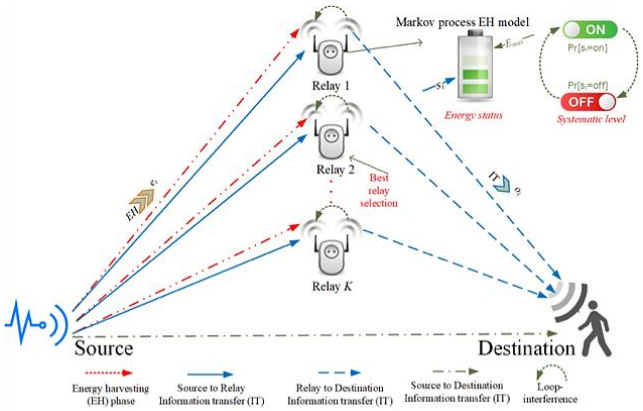

Figure 1. System models.

In addition, the carrier and symbol synchronization are assumed to be ideal. Each terminal knows beforehand its own channel state information (CSI). (S) is powered by a stable power source P_s and every (R) is powered by a battery P_R together with a EH module. The additive white Gaussian noise (AWGN), n_j, $(j \in \{R, D\})$ is with zero mean and variance N_0 at the (R_i) and (D), respectively.

In fact, the distances from (S) to (R_i), (R_i) to (D), and (S) to (D) are denoted with d_{SR_i}, d_{R_iD} and d_{SD}. Their corresponding channel coefficients are $l_{s,r}$, $l_{r,d}$, and $l_{s,d}$. As in Laourine et al. (2007), Mellios et al. (2014), (S) and (D) are HD and (R)s are FD. The FD setup causes the loop interference channel $l_{r,r}$ to the system. During the communication, which is split into time slots, the $i-$th relay $R_i (R_i \in C)$ is selected as per a (RS) scheme to help establishing the information transmission. Within a signal block, the narrow-band transmit signal at (S) is denoted as $s(t)$, (R_i) has zero mean, the statistical mean operation is denoted with $E[|s(t)|^2] = 1$.

We consider the random variables (RVs) which are independently and identically distributed (i.i.d) as per log-normal distribution as $l_{s,r}^2$, $l_{r,d}^2$, and $l_{s,d}^2$. The RVs are associated with parameters $LN(2\omega_{l_{s,r}}, 4\Omega_{l_{s,r}}^2)$, $LN\left(2\omega_{l_{r,d}}, 4\Omega_{l_{r,d}}^2\right)$, and $LN\left(2\omega_{l_{s,d}}, 4\Omega_{l_{s,d}}^2\right)$, respectively. Besides, the i.i.d loop interference channel following log-normal distribution $l_{r,r}^2$ is with parameter $LN(2\omega_{l_{r,r}}, 4\Omega_{l_{r,r}}^2)$. The loop interference strength given by this parameter is important for characterizing the performance of the FD system.

2.1. Standalone direct link

To serve as a foundation for further study, a direct transmission protocol, in which (S) transmits information directly to (D) without any assisting (R) in the LPEH WSNs is assumed and investigated.

Definition 1. In the context of direct transmission protocol, the direct (S)-(D) link is the unique option. Thus, it will use all the time slots from the signal block for data transmission.

Employing the direct transmission protocol, the overall (S)-(D) capacity can be obtained with zero-mean, circularly symmetric

$$C_{s,d} = W\left(1 + \frac{P_S}{N_0}\frac{|l_{s,d}|^2}{d_{s,d}^m}\right), \quad (1)$$

where m is the path loss exponent, and W is the frequency bandwidth.

As aforementioned, the ergodic OP is an indicator for evaluations of the system performance. This is the probability that the instantaneous capacity falls below a given threshold bits per channel use (BPCU) being R_0, and $Pr[C_{s,d} < R_0]$. Here, the probability density function (PDF) and the cumulative distribution function (CDF) of the RV X in log-normal distribution are respectively calculated by

$$F_X(z) = 1 - Q\left(\frac{\frac{10}{ln\ln(10)}ln\ln(z) - 2\omega_X}{2\Omega_X}\right), \quad (2)$$

and

$$f_X(z) = \frac{10/ln\ln(10)}{z\sqrt{8\pi\Omega_X^2}}e^{\left(-\frac{\left(\frac{10}{ln\ln(10)}ln\ln(z) - 2\omega_X\right)^2}{8\Omega_X^2}\right)}, \quad (3)$$

where $\xi = \frac{10}{ln\ln(10)}$ is a scaling constant and $Q(\cdot)$ is the Gaussian $Q-function, Q(x) = \int_x^\infty \frac{1}{\sqrt{2\pi}}e^{\left(-\frac{t^2}{2}\right)}dt$.

By utilizing the CDF of the log-normally distributed RV $|l_{s,d}|^2$ in (1), the ergodic OP for direct transmission protocol can be expressed as

$$OP_{s,d} = Pr\ Pr\left(|l_{s,d}|^2 < \left(2^{\frac{R_0}{W}} - 1\right)\frac{N_0 d_{s,d}^m}{P_s}\right)$$
$$= 1 - Q\left(\frac{\xi ln\ln(a) - 2\omega_{s,d}}{2\Omega_{s,d}}\right), \quad (4)$$

where $a = \frac{\gamma_0 N_0}{P_S d_{s,d}^{-m}}, and\ \gamma_0 = 2^{R_0/W} - 1.$

2.2. Relay-aided cooperative protocol

As aforementioned, the relay-aided cooperative protocol is deployed to improve the LPEH WSN performance.

Definition 2. In the context of relay-aided cooperative protocol, all the relay links can alternatively transmit the data in place of the direct link. Specifically, if the direct link is severely attenuated, a relay will be chosen among $\mathbf{K_s}$ from the cluster (C) to realize the data transmission alternatively. This is done on a condition that the relay has enough energy to conduct the task. This process is shown below in Fig. 2.

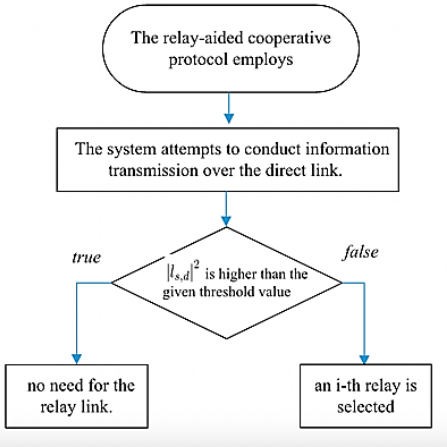

Figure 2. Criteria for relay selection.

By this approach, more time slots are saved, and overhead information is reduced, because only the needed relay link is activated. Besides, in LPEH WSN, we can receive the maximal diversity gain equaling the relay nodes that are available in the network, as proven in Laneman et al. (2004).

As described in Nguyen et al. (2018), one transmission cycle from (S) to (D) realized within T time is splitted into three slots as per the TSR protocol. The first time slot τT, where τ is the EH time factor, $(0 \leq \tau \leq 1)$, is spent by (R) to harvest the energy from the signal that (S) broadcasts. The remaining $(1-\tau)T$ is halved with one half for information of $(S)-(R_i)$ and the other for $(R_i)-(D)$.

Within τT, given the energy harvested the i −th (R) has harvested, $E_H = \frac{\eta\tau T P_s |l_{s,r_i}|^2}{d_{s,r_i}^m}$, the power that the relay transmits can be described as

$$P_{R_i} = \frac{E_H}{(1-\tau)T} = \frac{\eta\tau P_s |l_{s,r_i}|^2}{(1-\tau)d_{s,r_i}^m}, \quad (5)$$

where the EH efficiency $\eta, 0 \leq \eta \leq 1$, shows the circuitry's characteristics.

As mentioned in Zhong et al. (2014), as a relay can recognize its own signal in the FD multi-relay scenario, the interference cancellation can be applied to itself.

For $(1-\tau)T$, the signal after the interference cancellation at the i −th (R) can be expressed as

$$y_r(t) = \sqrt{\frac{P_s}{d_{s,r_i}^m}} l_{s,r_i} s(t) + \widehat{l_{r,r}} \hat{r}(t) + n_r, \quad (6)$$

where the information signal $s(t)$ is normalized as $E[|s(t)|^2] = 1$. The imperfect interference cancellation leaves out the residual loop interference $\widehat{l_{r,r}}$, and $E|\hat{r}(t)|^2 = P_{R_i}$.

In a FD-AF system, after the signal is base-band processed at (R_i) as per (6), it is amplified and then sent to (D). Therefore, (D) receives the signal of

$$y_d(t) = \sqrt{\frac{P_s P_{R_i}}{d_{s,r_i}^m d_{r_i,d}^m}} l_{s,r_i} l_{r_i,d} G s(t) + \sqrt{\frac{P_{R_i}}{d_{r_i,d}^m}} l_{r_i,d} l_{r,r} G r(t) + \sqrt{\frac{P_{R_i}}{d_{r_i,d}^m}} l_{r_i,d} G n_r + n_d, \quad (7)$$

where the relay gain, G, denotes the instantaneous received power normalization, within which process the relay transmission is allowed with maximum power, $P_s \rightarrow$, according to Tutuncuoglu et al. (2017).

$$G = \frac{1}{\sqrt{\frac{P_s}{d_{s,r_i}^m} |l_{s,r_i}|^2 + |\widehat{l_{s,r_i}}|^2 P_{R_i} + N_0}} \approx \frac{1}{\sqrt{\frac{P_s}{d_{s,r_i}^m} |l_{s,r_i}|^2 + |\widehat{l_{s,r_i}}|^2 P_{R_i}}}. \quad (8)$$

Then, (8) is substituted into (7) and modified so that the end-to-end SNR of the i −th (R) at (D) can be obtained

$$\gamma_{s,R_i,d} = \frac{\frac{P_s \gamma_{S,R_i}}{P_{R_i}\gamma_{R,R_i}} P_{R_i} \gamma_{R_i,D}}{\frac{P_s \gamma_{S,R_i}}{P_{R_i}\gamma_{R,R_i}} + P_{R_i}\gamma_{R_i,D} + 1}, \quad (9)$$

where $\gamma_{S,R_i} = |l_{s,r_i}|^2 d_{s,r_i}^{-m}$, $\gamma_{R_i,D} = |l_{r_i,d}|^2 d_{r_i,d}^{-m}$, and $\gamma_{R,R_i} = |l_{r,r}|^2$.

Additionally, the instantaneous capacity of the FD-AF-TSR system can be calculated.

$$C_{s,R_i,d} = (1-\tau)\left(1 + \gamma_{s,R_i,d}\right). \quad (10)$$

From here, the RS scheme for the in-studied LPEH WSN so-called the optimal loop interference relay selection (OPLIRS) scheme is derived. In particular, the OPLIRS scheme chooses first the (R) having the best end-to-end link, then updates the SINR in the first branch. Thus, the selected k relay, with $P_s \rightarrow$, has the condition of

$$k \approx arg\ arg \left\{\frac{P_s \gamma_{S,R_i}}{P_{R_i}\gamma_{R,R_i}}, P_{R_i}\gamma_{R_i,D}\right\}. \quad (11)$$

It should be noted that the OPLIRS scheme is established only if the full CSI is known.

2.3. Energy storage modeling at relay

The stationary stochastic process in Tutuncuoglu et al. (2017) states that the minimum energy needed to activate R_k and the harvested energy within the k −th signal block as en_k. Firstly, the R_k is assumed without energy storage, thus, operates only with en_k. The R_k runs out of energy if $en_k \leq P_{R_k}$. The probability that this event happens is named energy-exhausted probability and can be formulated as below.

$$OP_k = Pr[en_k < P_{R_k}] = \int_0^{P_{R_k}} f_{en_k}(x)dx, \quad (12)$$

where $f_{en_k}(x)$ is used to signify the PDF of the stationary stochastic process e_k.

In practice, however, the R_k is installed with a battery with capacity of en_{max}. The k −th signal block transmission consumes an amount of ou_k energy. As per the condition in Definition. 2, the ou_k can be expressed with the stationary random function as

$$Pr(ou_k) = \{OP_{s,d}/K, if\ Pr(ou_k = P_{R_k})\ 1 - OP_{s,d}/K, if Pr(ou_k = 0)\ 0,\ otherwise \quad (13)$$

where K denotes that every (R_k) can be activated with an equal probability. Notably, the variables en_k and ou_k are stationary and independent.

Additionally, to formulate the energy buffer status as per the Markov stochastic process, we use the denotation s_k, which stands for the initial energy amount the (R_k) stores before starting the k −th signal block transmission.

Subsequently, we can combine (12), (13) and the original PDF of en_k to obtain the stationary PDF of s_k being $f_{s_k}(x)$. Theoretically, all the stochastic characteristics of the EH module can be described with $f_{s_k}(x)$. However, because it is not necessary to include all these energy buffer statuses in the herein system, a simplified model is proposed. Specifically, according to Definition 2, the number of statuses is reduced to two processing steps and described below in Lemma 1.

Lemma. 1 The s_k and the possible energy that can be consumed at (R_k) are compared to make the decision on whether the transmission should be realized on the direct or the relaying link. This is shown below in Fig. 3.

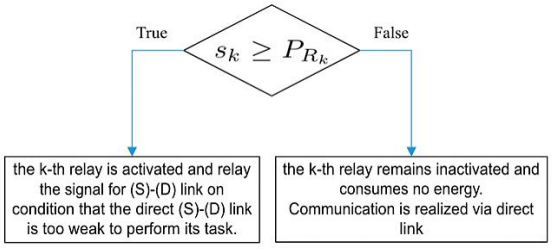

Figure 3. Criteria for choosing the direct or relaying link for information transmission.

These two statuses are therefore used to characterize the flow of the energy that has been harvested. Accordingly, we proposed an on-off $(1/0)$ model with denotation s'_k, which is described in Fig. 1. Then, we use the stationary PDF of s_k, $f_{s_k}(x)$ to formulate the stationary PDF of s'_k as follows.

$$Pr(s'_i) = \{\int_{P_{R_k}}^{en_{max}} f_{s_k}(x)dx,\ if\ Pr(s'_i = 1)\ \int_0^{P_{R_k}} f_{s_k}(x)dx,\ otherwise \quad (14)$$

Remarkably, (14) is not the same as the original PDF $f_{en_k}(x)$ of the harvested energy in (13).

Subsequently, an on−off $(1/0)$ (on/off status) model to describe the harvested energy flow have been formulated and described in the following *Remark 1*. For more details on the derivation, one can refer to Gorlatova et al. (2011, 2013).

Remark 1. The relaying link in LPEH WSN can be activated if the direct link cannot perform the information transmission task and the available energy stored at the relay is greater than $\mathrm{P_{R_k}}$. Additionally, thanks to the two parameters $\mathrm{P_{R_k}}$ and $\mathrm{OP_k}$, which characterize the EH module employed in $\mathrm{R_k}$, we can capture the stochastic property of the energy harvested beforehand with no loss.

3. Performance analysis

3.1. Formulating the problem

In practice, the relaying link over R_k cannot always be established due to deep fading or energy exhausting when the surrounding energy resources fluctuate. This event is named overall outage event and can be caused by three reasons as follows.

- At least one of the data packets cannot be successfully delivered during the information transmission from (S) to (D). This leads to the direct link's end-to-end SNR below the threshold value of the system.
- The energy harvested by R_k is not sufficient, so it cannot be activated to realize the information transmission via the relaying link. This is the so-called energy-exhausted probability.
- The relay R_k is activated, but cannot transfer all the data packets successfully. With sufficient energy amount from EH process. This leads to the relaying link's end-to-end SNR below the threshold value of the system.

Having acknowledged the above constraints, for the herein study, we assume that R_k possesses a sufficient amount of energy to realize the information transmission. Subsequently, the overall ergodic OP of the FD-AF-TSR LPEH WSN described in Definition. 2 can be formulated as follows.

$$OP_{oc} = OP_{s,d} \times \prod_{k=1}^{K} [OP_k + (1 - OP_k) \times OP_{s,R_k,d}]. \quad (15)$$

3. 2. Overall ergodic outage probability analysis

Regarding (10), the ergodic OP for S$-R_k-$D link can be fully defined as

$$OP_{s,R_k,d} = Pr\left\{\frac{\frac{P_S\gamma_{S,R_k}}{P_{R_k}\gamma_{R,R_k}}P_{R_k}\gamma_{R_k,D}}{\frac{P_S\gamma_{S,R_k}}{P_{R_k}\gamma_{R,R_k}}+P_{R_k}\gamma_{R_k,D}+1} < \gamma_1\right\}, \quad (16)$$

where $\gamma_1 = 2^{R_0/(1-\tau)W} - 1$.

Proposition 1.

The SNR in (11) is assumed to be high and identical. Thus, we can formulate the corresponding overall ergodic OP for the high SNR range under OPLIRS scheme as

$$OP_{oc}(\gamma_1) = \left[1 - Q\left(\frac{\xi\, ln\, ln\,(a)\, - 2\omega_{l_{s,d}}}{2\Omega_{l_{s,d}}}\right)\right] \times \left[OP_k + (1 - OP_k) \times OP_{s,R_k,d}(\gamma_1)\right]^K, \quad (17)$$

were

$$OP_{s,R_k,d}(\gamma_1) = 1 - Q\left(\frac{\xi ln ln\left(\frac{\eta\tau}{1-\tau}\gamma_1\right)+2\omega_{l_{r,r}}}{2\Omega_{l_{r,r}}}\right) \times Q\left(\frac{\xi ln ln\,(c) - 2\left(\omega_{l_{s,r}}+\omega_{l_{r,d}}\right)}{\sqrt{2}\left(\Omega_{l_{s,r}}+\Omega_{l_{r,d}}\right)}\right), a = \frac{(1-\tau)}{\eta\tau P_s}\gamma_1.$$

Proof:

It is worth noting that the γ_{R_k} in (11) is crucial for the RS process. As we combine (5) and (6), we can formulate the SNR at (R) as follows.

$$\gamma_{S,R_k} = \frac{P_S\gamma_{S,R_k}}{P_{R_k}} = \frac{1-\tau}{\eta\tau} \times \frac{1}{\gamma_{R,R_k}}. \quad (18)$$

Similarly, the SNR at (D) is given by.

$$\gamma_{R_k,D} = P_{R_k}\gamma_{R_k,D} = \frac{\eta\tau\, P_S}{(1-\tau)}\gamma_{S,R_k}\gamma_{R_k,D}. \quad (19)$$

Subsequently, we combine (18) and (19) then substitute them into (11) to obtain the ergodic OP in (16), considering R_k, as follows

$$OP_{s,R_k,d} = Pr\left\{\left\{\frac{1-\tau}{\eta\tau Y}, \frac{\eta\tau P_S X}{(1-\tau)}\right\} < \gamma_1\right\}, \quad (20)$$

where $X = \gamma_{S,R_k}\gamma_{R_k,D}$ and $Y = \gamma_{R,R_i}$.

It should be noted that all the aforementioned channels means and variances are i.i.d. as per the log-normal distribution . Assuming that X and Y are two independent RVs, the ergodic OP of the system with the OPLIRS scheme in (11) can be expressed as

$$OP_{s,R_k,d} = 1 - \underline{F_Y}\left(\frac{\eta\tau}{1-\tau}\gamma_1\right)\underline{F_X}\left(\frac{(1-\tau)}{\eta\tau P_S}\gamma_1\right), \quad (21)$$

where $\underline{F_Y}(.)$ and $\underline{F_X}(.)$ are the complementary CDFs of Y and X. Because the RV Y is distributed in a log-normal manner, its complementary CDF $\underline{F_Y}(.)$ can be obtain with ease as follows.

$$\underline{F_Y}\left(\frac{\eta\tau}{1-\tau}\gamma_1\right) = Q\left(\frac{\xi ln ln\left(\frac{\eta\tau}{1-\tau}\gamma_1\right)+2\omega_{l_{r,r}}}{2\Omega_{l_{r,r}}}\right). \quad (22)$$

Besides, the RV X is a product of two RVs which are as well log-normally distributed, its complementary CDF can be obtained as.

$$\underline{F_X}\left(\frac{(1-\tau)}{\eta\tau P_S}\gamma_1\right) = Q\left(\frac{\xi ln ln\left(\frac{(1-\tau)}{\eta\tau P_S}\gamma_1\right)-2\left(\omega_{l_{s,r}}+\omega_{l_{r,d}}\right)}{\sqrt{2}\left(\Omega_{l_{s,r}}+\Omega_{l_{r,d}}\right)}\right). \quad (23)$$

As we substitute (22) and (23) into (21), the ergodic OP can be obtained as.

$$OP_{s,R_k,d} = 1 - Q\left(\frac{\xi ln ln\left(\frac{\eta\tau}{1-\tau}\gamma_1\right)+2\omega_{l_{r,r}}}{2\Omega_{l_{r,r}}}\right) \times Q\left(\frac{\xi ln ln\left(\frac{(1-\tau)}{\eta\tau P_S}\gamma_1\right)-2\left(\omega_{l_{s,r}}+\omega_{l_{r,d}}\right)}{\sqrt{2}\left(\Omega_{l_{s,r}}+\Omega_{l_{r,d}}\right)}\right) \quad (24)$$

Consequently, (24) and (4) are substituted into (15) to obtain the overall ergodic OP in OPLIRS scheme, as given in (17).

4. Results and discussion

In this section, the Monte Carlo numerical simulation was conducted to investigate the overall ergodic OP of the in-studied system with OPLIRS scheme. The system parameters for the simulations are listed below in Table. 1. The results are calculated based on proposition 1 in (17), by means of MATLAB simulation.

Fig. 4 illustrates the overall ergodic OP versus the EH time switch τ. Two values of loop interference channel variance being $\Omega_{l_{r,r}} = 2(dB)$ and 4(dB) are used together with the constant power source of $P_s = 5$ (dB). It is possible to observe that the two curves reach their minimum at $\tau = (0.175)$, at which the system performs the best and the coding gap is the largest. As τ increases to over 0.3, the overall ergodic OP curves exponentially decrease corresponding to the extreme case when too much time is dedicated for the EH activity resulting in insufficient time for data transmitting purpose.

Table 1. Simulation parameters.

Primary Parameters	Description	Values
OP_k	energy-exhausted probability	10^{-1}
W	frequency bandwidth	2(W)
R_0	transmission rate threshold	2(bps/Hz)
P_s	traditional stabilized power source	5(dB)
N_0	overall AWGNs	1
η	EH efficiency	1
τ	EH time fraction	0.2
m	path-loss exponent	2
$d_{s,r}$	(S)- (R_k) distance	5(m)
$d_{r,d}$	(R_k)-(D) distance	5(m)
$d_{s,d}$	(S)-(D) distance	10(m)
$\Omega_{l_{s,r}}$	(S)- (R_k) channel mean	4(dB)
$\Omega_{l_{r,d}}$	(R_k)-(D) channel mean	4(dB)
$\Omega_{l_{s,d}}$	(S)--(D) channel mean	4(dB)
$\Omega_{l_{r,r}}$	loop interference (R_k) channel mean	2(dB)
$\omega_{l_{s,r}}$	(S)- (R_k) channel variance	3(dB)
$\omega_{l_{r,d}}$	(S)--(R_k)-(D) channel variance	3(dB)
$\omega_{l_{s,d}}$	(S)-(D) channel variance	3(dB)
$\omega_{l_{r,r}}$	loop interference (R_k) channel variance	3(dB)

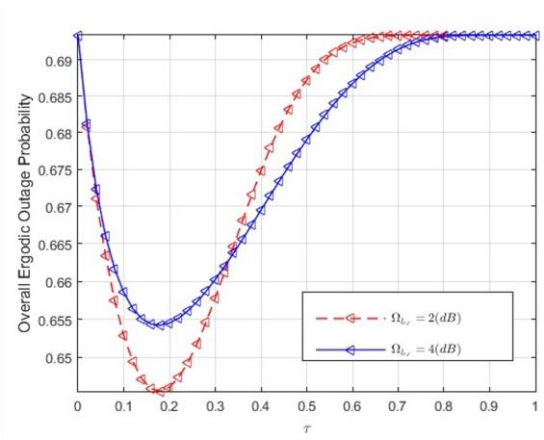

Figure 4. Relation between the overall ergodic OP and EH time switch τ, with two $\Omega_{l_{r,r}}$ values.

Fig. 5 depicts the relation between the overall ergodic OP of the LPEH WSN and the SNR. For comparison, we use three values of 0, 0.5 and 1 for the energy-exhausted probability OP of best RS. The $OP_k = 0$ when the LPEH WSN operates with the cooperative relays, $OP_k = 1$ with direct link, and $OP_k = 0.5$ for both or only the relay link (red color). It can be noted that as SNR increases from -20 to 30 dB, the $OP_k = 0.5$ without direct link delivers the highest overall ergodic OP, thus, the worst system perform. The remaining curves are relatively close to another and they sharply approach 0 overall ergodic OP when SNR increases to 30(dB). The theory and simulation agree well with each other suggest that the importance of implementing the EH cooperative relays in boosting the performance of the LPEH WSN.

Fig. 6 plots the overall ergodic OP versus the SNR when changing the number of relays, K, from 1 to 3 and 5. The three curves are simulated with $OP_k = 10^{-1}$. It is quite intuitive that the more intermediate relays are installed, the lower the overall ergodic OP curve, leading to the better system performance. Remarkably, changing the number of relays results in the performance curves with similar shape as changing the OP_k value. So far, it can be concluded that utilization of the intermediate EH relays is beneficial for the LPEH WSNs with OPLIRS, and the higher the number of relays, the better the system performs.

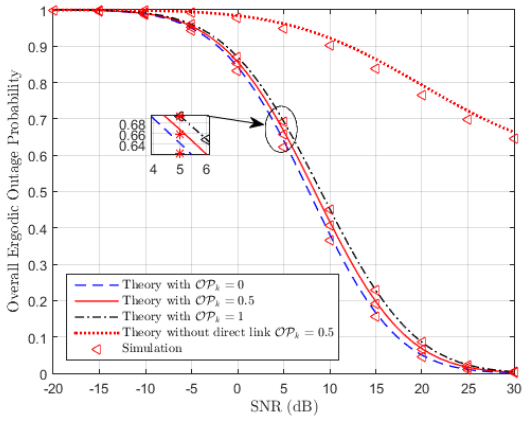

Figure 5. Relation between the overall ergodic OP and the SNR, with three OP_k values.

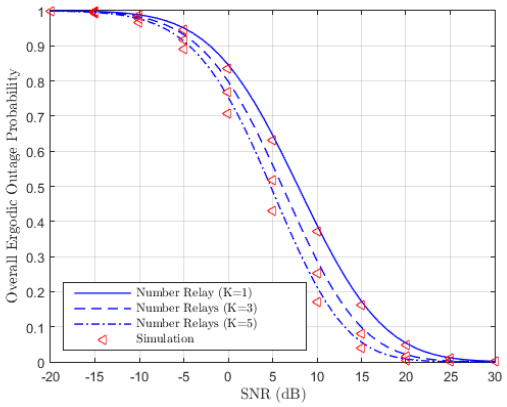

Figure 6. Relation between the overall ergodic OP and the SNR, with three K values.

5. Conclusions

In general, the paper presents the performance analysis in terms of the overall ergodic OP of the OPLIRS scheme in the context of LPEH WSN. Because the simulations correlate well with the theory, the expressions that we derived show the potential to be applicable for other future studies. It is as well proven that the log-normal fading channel is appropriate for modelling such indoor scenarios. Future studies can consider different RS schemes and compare them with the herein studies to find the best one for the LPEH WSN setup.

Conflict of interest

The authors have no conflict of interest to declare.

Acknowlegements

This researh is funded by Thu Dau Mot University under grant number DT20.2-020.

Funding

This research is funded by Thu Dau Mot University under grant number DT.20.2-020.

References

Assogba, O., Mbodji, A. K., & Diallo, A. K. (2020). Efficiency in RF energy harvesting systems: A comprehensive review. In *2020 IEEE International Conf on Natural and Engineering Sciences for Sahel's Sustainable Development-Impact of Big Data Application on Society and Environment (IBASE-BF)* (pp. 1-10). IEEE. https://doi.org/10.1109/IBASE-BF48578.2020.9069597

Cheng, X., Cao, R., & Yang, L. (2013). Relay-aided amplify-and-forward powerline communications. *IEEE Transactions on Smart Grid*, *4*(1), 265-272. https://doi.org/10.1109/TSG.2012.2225645

da Costa, D. & Aissa, S. (2010). Performance analysis of relay selection techniques with clustered fixed-gain relays. *IEEE Signal Processing Letters*, *17*(2), 201-204. https://doi.org/10.1109/LSP.2009.2036880

Ezzine, S., Abdelkefi, F., Cances, J. P., Meghdadi, V., & Bouallégue, A. (2015, May). Capacity analysis of an OFDM-based two-hops relaying PLC systems. In *2015 IEEE 81st Vehicular Technology Conference (VTC Spring)* (pp. 1-5). IEEE. 5. https://doi.org/10.1109/VTCSpring.2015.7145725

Foschini, G. J. (2002). Layered space-time architecture for wireless communication in a fading environment when using multi-element antennas. *Bell Labs Technical Journal*, *1*(2), 41-59. https://doi.org/10.1002/bltj.2015

Georgiou, O., Mimis, K., Halls, D., Thompson, W. H., & Gibbins, D. (2016). How many wi-fi aps does it take to light a lightbulb? IEEE Access, 4, 3732-3746. https://doi.org/10.1109/ACCESS.2016.2573681

Gorlatova, M., Wallwater, A., & Zussman, G. (2011). Networking low-power energy harvesting devices: Measurements and algorithms. In *IEEE 2011 Proceedings IEEE INFOCOM*. https://doi.org/10.1109/INFCOM.2011.5934952

Gorlatova, M., Wallwater, A., & Zussman, G. (2013). Networking low-power energy harvesting devices: Measurements and algorithms. IEEE Transactions on Mobile Computing, 12(9):1853-1865. https://doi.org/10.1109/TMC.2012.154

Laneman, J., Tse, D., & Wornell, G. (2004). Cooperative diversity in wireless networks: Efficient protocols and outage behavior. IEEE Transactions on Information Theory, *50*(12), 3062-3080. https://doi.org/10.1109/TIT.2004.838089

Laourine, A., Stephenne, A., & Affes, S. (2007). Estimating the ergodic capacity of log-normal channels. *IEEE Communications Letters*, *11*(7), 568-570. https://doi.org/10.1109/LCOMM.2007.070302

Li, T., Fan, P., & Letaief, K. B. (2016). Outage probability of energy harvesting relay-aided cooperative networks over rayleigh fading channel. IEEE Transactions on Vehicular Technology, *65*(2), 972-978. https://doi.org/10.1109/TVT.2015.2402274

Liu, H., Kim, K. J., Kwak, K. S., & Poor, H. V. (2016). Power splitting-based SWIPT with decode-and-forward full-duplex relaying. *IEEE Transactions on Wireless Communications*, *15*(11), 7561-7577. https://doi.org/10.1109/TWC.2016.2604801

Mellios, E., Goulianos, A., Dumanli, S., Hilton, G., Piechocki, R., & Craddock, I. (2014). Off-body channel measurements at 2.4 GHz and 868MHz in an indoor environment. *In Proceedings of the 9th International Conference on Body Area Networks*. ICST. https://doi.org/10.4108/icst.bodynets.2014.257000

Nguyen, H.-S., Ly, T., Nguyen, T.-S., Huynh, V., Nguyen, T.-L., & Voznak, M. (2019). Outage performance analysis and SWIPT optimization in energy harvesting wireless sensor network deploying NOMA. Sensors, *19*(3), 613. https://doi.org/10.3390/s19030613

Nguyen, H.-S., Nguyen, T.-S., & Voznak, M. (2018). Relay selection for SWIPT: Performance analysis of optimization problems and the trade-off between ergodic capacity and energy harvesting. AEU - *International Journal of Electronics and Communications*, 85, 59-67. https://doi.org/10.1016/j.aeue.2017.12.012

Perera, T. D. P., Jayakody, D. N. K., Sharma, S. K., Chatzinotas, S., & Li, J. (2018). Simultaneous wireless information and power transfer (SWIPT): Recent advances and future challenges. *IEEE Communications Surveys & Tutorials*, *20*(1), 264-302. https://doi.org/10.1109/COMST.2017.2783901

Pu, H., Liu, X., Zhang, S., & Xu, D. (2019). Adaptive cooperative non-orthogonal multiple access-based power line communication. *IEEE Access*, 7, 73856-73869. https://doi.org/10.1109/ACCESS.2019.2920244

Ramesh, R., Gurugopinath, S., & Muhaidat, S. (2020). Outage performance of relay-assisted NOMA over power line communications. In *2020 IEEE 31st Annual International Symposium on Personal, Indoor and Mobile Radio Communications* (pp. 1-6). IEEE. https://doi.org/10.1109/PIMRC48278.2020.9217345

Rabie, K. M., Adebisi, B., Gacanin, H., & Yarkan, S. (2018). Energy-per-bit performance analysis of relay-assisted power line communication systems. *IEEE Transactions on Green Communications and Networking*, 2, 360-368. https://doi.org/10.1109/TGCN.2018.2794613

Rabie, K. M., Adebisi, B., Yousif, E. H. G., Gacanin, H., & Tonello, A. M. (2017). A comparison between orthogonal and non-orthogonal multiple access in cooperative relaying power line communication systems. *IEEE Access*, 10118-10129. https://doi.org/10.1109/ACCESS.2017.2710280

Rabien, K. M., Adebisi, B., & Salem, A. (2016). Improving energy efficiency in dual-hop cooperative plc relaying systems. *In 2016 International Symposium on Power Line Communications and its Applications (ISPLC)*, 196-200. https://doi.org/10.1109/ISPLC.2016.7476262

Renzo, M. D., Graziosi, F., & Santucci, F. (2008). Performance of cooperative multi-hop wireless systems over log-normal fading channels. In *IEEE GLOBECOM 2008 IEEE Global Telecommunications Conference*, 1-6. https://doi.org/10.1109/GLOCOM.2008.ECP.861

Renzo, M. D., Graziosi, F., & Santucci, F. (2010). A comprehensive framework for performance analysis of cooperative multi-hop wireless systems over log-normal fading channels. IEEE Transactions on Communications, *58*(2), 531-544. https://doi.org/10.1109/TCOMM.2010.02.080273

Riihonen, T., Werner, S., & Wichman, R. (2011). Mitigation of loopback self-interference in full-duplex MIMO relays. *IEEE Transactions on Signal Processing*, *59*(12), 5983-5993. https://doi.org/10.1109/TSP.2011.2164910

Rubin, I., Lin, Y.-Y., & Kofman, D. (2014). Relay-aided networking for power line communications. *In 2014 IEEE Information Theory and Applications Workshop (ITA)*. https://doi.org/10.1109/ITA.2014.6804270

Salem, A., Hamdi, K. A., & Alsusa, E. (2017). Physical layer security over correlated log-normal cooperative power line communication channels. *IEEE Access*, 5, 13909-13921. https://doi.org/10.1109/ACCESS.2017.2729784

Sidhu, R. K., Ubhi, J. S., & Aggarwal, A. (2019). A survey study of different RF energy sources for RF energy harvesting. In 2019 IEEE International Conference on Automation, *Computational and Technology Management (ICACTM)*. https://doi.org/10.1109/ICACTM.2019.8776726

Tutuncuoglu, K., Ozel, O., Yener, A., & Ulukus, S. (2017). The binary energy harvesting channel with a unit-sized battery. *IEEE Transactions on Information Theory*, *63*(7),4240-4256. https://doi.org/10.1109/TIT.2017.2690997

Wang, H., Ma, S., Ng, T.-S., & Poor, H. V. (2011). A general analytical approach for opportunistic cooperative systems with spatially random relays. *IEEE Transactions on Wireless Communications*, *10*(12), 4122-4129. https://doi.org/10.1109/TWC.2011.093011.101386

Wu, X. (2015). *Reliable indoor power line communication systems: via application of advanced relaying processing* (Doctoral dissertation, Curtin University). http://hdl.handle.net/20.500.11937/454

Zeng, Y. & Zhang, R. (2015). Full-duplex wireless-powered relay with self-energy recycling. *IEEE Wireless Communications Letters, 4*(2), 201-204. https://doi.org/10.1109/LWC.2015.2396516

Zhang, Z., Chai, X., Long, K., Vasilakos, A. V., & Hanzo, L. (2015). Full duplex techniques for 5g networks: self-interference cancellation, protocol design, and relay selection. *IEEE Communications Magazine*, *53*(5),128-137. https://doi.org/10.1109/MCOM.2015.7105651

Zhang, Z., Zhang, W., & Tellambura, C. (2009). Cooperative OFDM channel estimation in the presence of frequency offsets. *IEEE Transactions on Vehicular Technology, 58*(7), 3447-3459 https://doi.org/10.1109/TVT.2009.2016345

Zhong, C., Suraweera, H. A., Zheng, G., Krikidis, I., and Zhang, Z. (2014). Wireless information and power transfer with full duplex relaying, *IEEE Transactions on Communications*, *62*(10), 3447-3461. https://doi.org/10.1109/TCOMM.2014.2357423

Zhu, B., Cheng, J., Yan, J., Wang, J., Wu, L., & Wang, Y. (2017). A new technique for analyzing asymptotic outage performance of diversity over lognormal fading channels. *In 2017 15th Canadian Workshop on Information Theory (CWIT)* (pp. 1-5). IEEE. https://doi.org/10.1109/CWIT.2017.7994815